Friction factor from velocity profiles in smooth turbulent channel flows

Hélène PAYET-TAILLE[1], *Stéphane* MARCHANDON[1*], and *Rafik* ABSI[2†]

[1] EBI, EBInnov-Lab, 9 avenue des Genottes, CS 90009, 95895 Cergy cedex, France
[2] ECAM-EPMI, LR2E-Lab, Quartz-Lab (EA 7393), 13 boulevrad de l'Hautil, 95094 Cergy-Pontoise cedex, France

Abstract. Fluid dynamics plays an important role in many Renewable energies studies, i.e. wind and tidal turbines, wave energy geothermal and solar power, …). Friction factor f is an important parameter for the determination of pressure drop in different processes and systems. In this study, we use DNS data of turbulent smooth channels to evaluate different methods. First, a recalibration of Dean's correlation (Dean, 1978) is proposed. The aim of the study is to obtain accurate wall friction factors from velocity profiles. On the one hand, we obtained two implicit analytical relations based on the law-of-the-wall: a logarithmic friction relation similar to that of pipes and a linear-logarithmic friction relation. On the other hand, we obtained f from the computation of the average velocity. It is first calculated from the law-of-the-wall and allows a good prediction of f for $Re_\tau > 395$ but presents a gap for low Re_τwhich is related to inaccurate velocities. Low-Reynolds number effect in channel flows has been previously observed in different experimental and computational studies. In order to provide suitable friction factor values, it is important to predict velocities accurately on the overall channel height. We used therefore a more appropriate method which consists to use for $y^+ < 20$ the momentum equation with an eddy viscosity formulation (Absi, 2019) and the log-wake law for high y^+ values. This method provides accurate friction factor values and allows good agreement with DNS data.

1 Introduction

Computational fluid dynamics (CFD) represents an effective and usefull tool in many Renewable energies studies, (i.e. wind and tidal turbines, wave energy geothermal and solar power,…). Different processes and systems need the evaluation of energy losses. The pressure drop is involved in heat exchangers, chemical and petroleum processes, nuclear, refrigerating system, ventilation, heating [16]. It is also important in hydraulic engineering for the design of water systems. Relations were developed to provide the friction factor f. Some of them are empirical and others are based on more theoretical considerations. For pipes, the well-known Prandtl equation or PKN (Prandtl-Karman-Nikuradse) correlation for

* Corresponding author: s.marchandon@hubebi.com
† Corresponding author: r.absi@ecam-epmi.com

smooth turbulent pipes is based on the logarithmic velocity profile. However, it is possible to find different coefficients for this equation related to the used friction factor (Darcy or Fanning) and/or logarithm (base ten or e). Several authors proposed more accurate correlation based on recent experiments [10] [21] [23-24-25]. More advanced methods were used to propose accurate friction factor relations as artificial neural network [11]. The study of friction factor for channel flows is still lacking, contrary to pipe flows. We will consider the turbulent channel flow which is basically the flow between two horizontal plane plates located at $2h$ from each other. This represents an ideal theoretical framework and is related to most of the industrial applications. It was already studied experimentally [28] [30], theoretically, and numerically [22] [14-15] [27] [9] [1-8]. Currently, "direct numerical simulation" (DNS) provides accurate results [26] [20] [19] which are used extensively to evaluate and validate the different proposed relations. It is possible to obtain the friction factor from DNS data, by Reynolds Re and Reynolds friction Re_τ numbers, or through the average velocity based on velocity profiles. Reynolds numbers in many practical situations are several orders of magnitude higher than those from computational or laboratory experiments. Even for different data at different Reynolds numbers, when nondimensionalized using appropriate length and velocity scales, mean streamwise velocity profiles and other statistical turbulence quantities collapse to a single universal profile. In fully developed turbulent flows, we can distinguish the outer region from the inner or near-wall region which is composed by the viscous sublayer, the buffer layer and the overlap or log-law layer.

We will start the study by evaluating the Dean's correlation [13]; which provides a Re-dependent friction factor. The aim of this note is to evaluate the accuracy of skin friction factors obtained from velocity profiles. On the one hand, we will use the log-law on the overall height h, to obtain the logarithmic friction relation similar to that of pipes. Then, in order to improve this relation we will consider the linear profile in the viscous sublayer. On the other hand, the friction factor will be obtained from the average velocity based on the law-of-the-wall, the log-wake law [12] [18] or by solving the momentum equation.

2 Friction factor and velocity profiles

2.1 Friction factor

Fanning's friction factor is defined as:

$$f = \frac{\tau_p}{\frac{1}{2}\rho\, u_{moy}^2} \tag{1}$$

Where: τ_p is the wall shear stress, ρ the fluid density and u_{moy} the fluid average velocity on the channel height. By using wall units, we write:

$$f = \frac{2}{u_{moy}^{+2}} \tag{2}$$

With $u^+_{moy}=u_{moy}/u_\tau$ and $u_\tau=(\tau_p/\rho)^{0.5}$ is the friction velocity. The relation with the Darcy's factor λ

is given by: $f=(1/4)\lambda$. We can rewrite equation (2) as a function of Reynolds numbers: $Re=(2hu_{moy})/\nu$ and the friction Reynolds number defined as $Re_\tau = (h\, u_\tau)/\nu$. It is possible to write:

$$Re = 2u_{moy}^{+} Re_\tau \tag{3}$$

By substituting in equation (2), we obtain:

$$f = \frac{8Re_\tau^2}{Re^2} \tag{4}$$

This relation allows obtaining the friction factor f from Reynolds numbers when they are known, without the need of average velocity based on velocity profiles.
Dean [13] proposed a correlation which provides the friction factor as a function of the Reynolds number:

$$f = 0.073\, Re^{-0.25} \tag{5}$$

2.2 Average or Bulk velocity

The average velocity can be obtained by the following equations:

$$u_{moy} = \frac{1}{h}\int_0^h u dy$$

$$u^+_{moy} = \frac{1}{Re_\tau}\int_0^{Re_\tau} u^+ dy^+ \tag{6}$$

With: $u^+=u/u_\tau$, $y^+=(y\, u_\tau)/\nu$, for these equations we need to know the velocity profile which is given for the inner region by the law of the wall [17]:

- The linear profile in the viscous sublayer where $\nu \gg \nu_t$

$$u^+ = y^+ \tag{7}$$

- The logarithmic profile in the overlap or log-law layer where $\nu_t \gg \nu$

$$u^+ = \frac{1}{\kappa} ln(y^+) + B \tag{8}$$

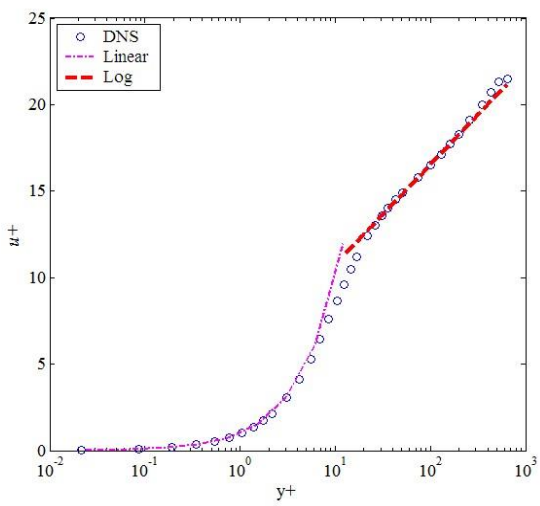

Fig. 1. Mean velocity profiles u+ = f(y+) for Re = 642.

Figure (1) presents linear and logarithmic profiles (equations 7 and 8) with DNS data for a friction Reynolds number Re_τ=642 [20]. For the logarithmic profile, we use $\kappa=0.4$ and $B=5$ which seem to be suitable. These approximations (curves of equations 7 and 8) are very close to DNS data. However, the velocities are not accurate near the intersection between the two velocity curves and also in the outer region for high y^+.

The aim of the study is to identify the most suitable method to obtain an accurate friction factor for different Reynolds numbers from velocity distribution. Different methods to obtain the friction factor based on equation (2) will be considered and evaluated by comparison with DNS data. These methods need the average velocity obtained from velocity profiles.

3 Evaluation of Dean's correlation by comparison with DNS data

We evaluate the Dean's correlation by comparison with the friction factor obtained from DNS data.

3.1 Determination of friction factor from DNS data

We obtain values of *f* from DNS by both Reynolds numbers (equation 4) or from the average velocity (equation 2).

f values obtained from Reynolds numbers:

In table (1), friction factor *f* is obtained from *Re* and Re_τ of DNS data (Iwamoto, 2002).

Table 1. Friction factor from DNS based on Re et Re_τ.

Re_τ	*Re*	$f\times10^{-3}$
109	3220.38	9.237
150	4586.21	8.612
298	10039.1	7.044
642	24272.2	5.606

f values obtained from the average velocities:

The trapezoidal rule solves the integral (equation 6) by approximating the region under the data and provides the area from elementary area for each Δy^+, as:

$$S_{totale} = \sum_{i=1}^{N}\left(\Delta y^+ \times \left(\frac{u_{i+1}^+ + u_i^+}{2}\right)\right)$$

Table 2. Friction factor from DNS based on u_{moy}^+.

Re_τ	*Total area*	u^+moy	*Re*	$f\times10^{-3}$
109	1610.02	14.77	3220.04	9.166
150	2293	15.28	4586	8.558
298	5010	16.82	10026.17	7.067
642	12125.44	18.88	24250.88	5.606
2003	43523.01	21.72	87046.03	4.235

For each Reynolds number we obtained the area which provides the average velocities u_{moy}^+ and therefore the friction factor (table 2).

This method is particularly interesting for Re_τ=2003 [19] where the Reynolds number is not provided and therefore we are unable to use the first method. However, for Iwamoto's data this second method allows a second estimation of *f*.

3.1 Comparison and proposition of a new calibration for Dean's correlation

Figure (2) shows that Dean's correlation (equation 5) does not provide accurate predictions of friction factor particularly for low Reynolds numbers. We will consider the DNS values in order to recalibrate this correlation which we write as: $f = a\ Re^{-b}$

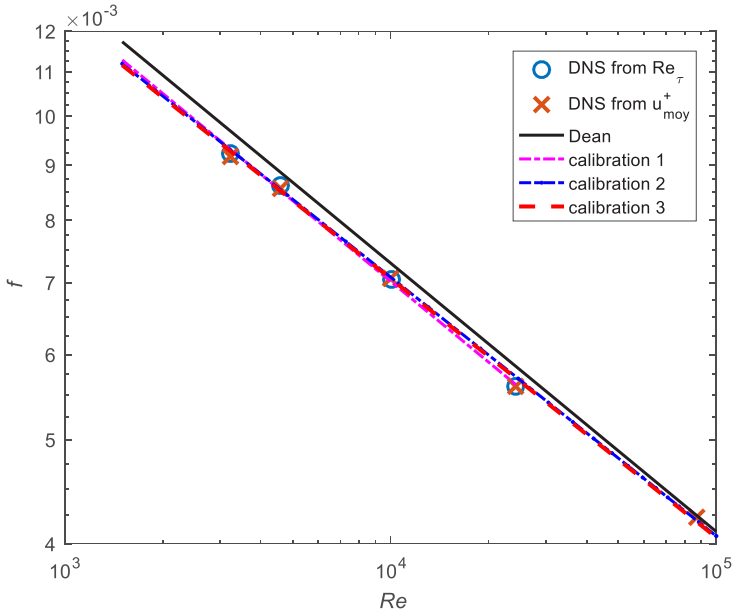

Fig. 2. Friction factor from Dean's correlation and DNS data.

Different calibrations are proposed: In the first, we use the values of *f* obtained from Re_τ of Iwamoto until 642 (Table 1), the coefficients are $a=0.0702$ and $b=0.25$. In the second, the calibration is based on *f* obtained from the average velocity (Table 2), we obtain $a=0.0652$ and $b=0.241$. Finally, the third calibration which seems the most adequate uses both the first for Iwamoto's data and the second for *Re*=2300, we obtain $a=0.065$ and $b=0.241$. The relation is therefore:

$$f = 0.065\, Re^{-0.241} \tag{9}$$

Figure (2) shows that this calibrated equation allows a more accurate prediction of the friction factor. Since equation (9) is an empirical relation, it is interesting to link the friction factor *f* to flow proprieties. In the following sections, we will find *f* from the velocity distribution.

4 Analytical relations for friction factor based on velocity laws

4.1 Logarithmic friction relation

In this approach, for the average velocity we assume a logarithmic profile within the overall height. From equation (6):

$$\frac{u_{moy}}{u_\tau} = \frac{1}{h}\int_0^h \frac{u}{u_\tau} dy = \frac{1}{h}\int_0^h \left[\frac{1}{\kappa} ln\left(\frac{y\, u_\tau}{\nu}\right) + B\right] dy \quad (10)$$

After integrating we obtain:

$$u^+_{moy} = \frac{u_{moy}}{u_\tau} = \frac{1}{\kappa}\ln(Re_\tau) - 1 + B \quad (11)$$

By this method, we obtain the friction factor from the average velocity as for pipes. Equations (2) and (4) provide $u^+_{moy} = (2/f)^{0.5}$ and $Re_\tau = (f/8)^{0.5}$, we obtain therefore :

$$\frac{1}{\sqrt{f}} = c_1 \ln\left(Re\sqrt{f}\right) + c_2 \quad (12)$$

We called equation (12) the logarithmic friction relation (LFR), with:

$c_1 = \frac{1}{\sqrt{2}\kappa}$ and $c_2 = -\frac{\ln(\sqrt{8})}{\sqrt{2}\kappa} - \frac{1/\kappa - B}{\sqrt{2}}$

With the values κ=0.4 et B=5, equation (12) can be expressed as a function of Re_τ:

$$\frac{1}{\sqrt{f}} = 1.77\ln(Re_\tau) + 1.77$$

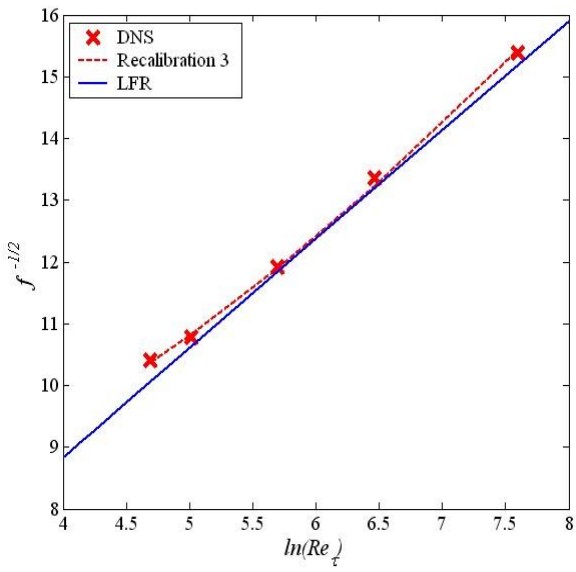

Fig. 3. Logarithmic friction factor and DNS data.

In figure (3), the logarithmic friction relation is compared to DNS data. It shows that with LFR, we obtain accurate friction factor *f* values for intermediate Re_τ. However, it presents a difference with DNS data for high and low Re_τ. This gap can be related to the used assumption of a velocity logarithmic profile on the overall height. Indeed, the integration provides mistakes related to the inaccuracy of the logarithmic profile for both low and high values of y^+ (figure 1). A more accurate average velocity needs more appropriate assumptions for velocity profile. In order to improve the logarithmic friction relation, it seems to be more suitable to take into account the linear profile in addition to the logarithmic profile (figure 1).

4.2 Linear-logarithmic friction relation

In order to improve the former analytical relation for the friction factor, we assume a linear profile until $y^+ = 11.5$ and the logarithmic profile for $y^+ > 11.5$. The value of $y^+ = 11.5$ represents approximately the intersection between linear and logarithmic velocity profiles (figure 1). This assumption allows to obtain the average velocity and therefore the following equation for f:

$$\frac{1}{\sqrt{f}} = \underbrace{\boxed{\frac{1}{\sqrt{2}\kappa}\ln(Re_\tau) - \frac{1/\kappa - B}{\sqrt{2}}}}_{\text{Term I}} + \underbrace{\boxed{\frac{8{,}13}{Re_\tau}\left[5{,}75 - \frac{1{,}44}{\kappa} - B\right]}}_{\text{Term II}} \tag{13}$$

Equation (13) is the linear-logarithmic friction relation (LLFR), where the first term is the logarithmic friction relation and the second term results from the use of the linear profile for $y^+ > 11.5$.

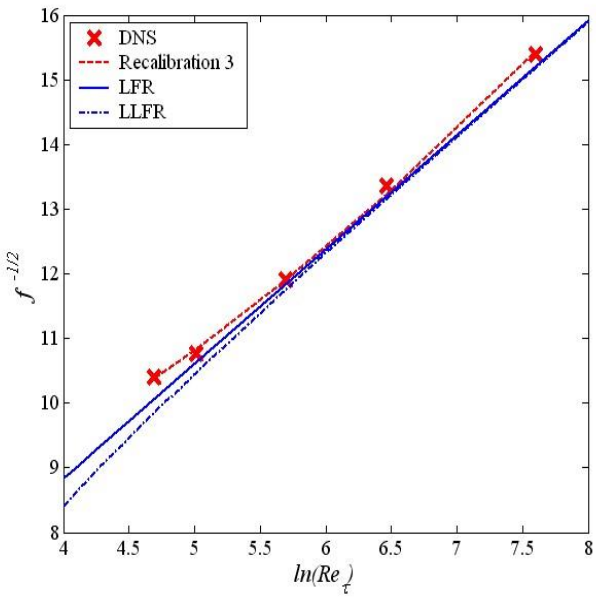

Fig. 4. Logarithmic and Linear-Logarithmic friction relations and DNS data.

Figure (4) shows an unexpected behavior: LLFR is more distant from the DNS data than LFR for low Re_τ. Figure (5) presents an explanation through a comparison between the used assumptions for both friction relations (logarithmic and linear-logarithmic). The assumption of a logarithmic velocity profile on the overall height (figure 5.a) shows for Re_τ=109 two potential mistakes: the first for $y^+<20$ and the second for $y^+>20$. The logarithmic velocity profile doesn't take into account the region in figure (5.a) represented by vertical lines and considers the region with horizontal lines. However, this mistake seems to have little consequence since both effects are somewhat balanced.

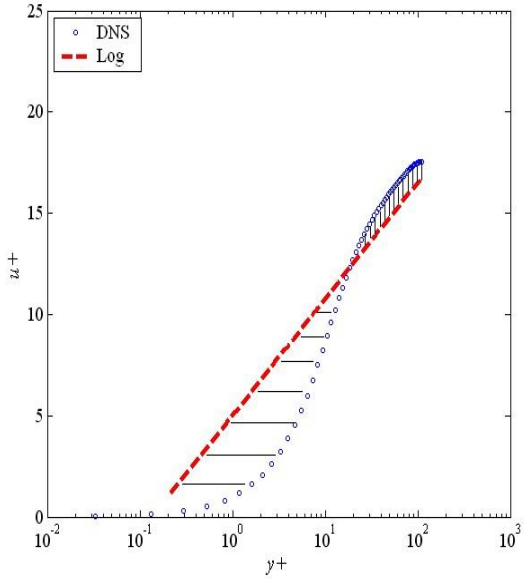

(a)

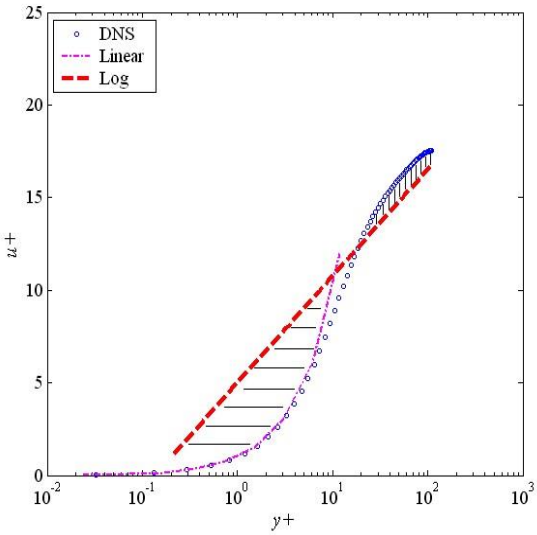

(b)

Fig. 5. Comparison of the assumptions for both friction relations (logarithmic and linear-logarithmic); a) logarithmic velocity profile and DNS data, b) linear and logarithmic velocity profiles and DNS data.

However, even if the linear-logarithmic relation is more realistic, the result is less accurate. This seems to be related to the region with horizontal lines for y+>11.5 (figure 5.b) which is not considered anymore. This reduces therefore the former balance with the region represented by vertical lines.

4.3 Summary of analytical relations

These analytical relations present two shortcomings:

- Both analytical relations are implicit
- Results differ from DNS for low and high Re_τ

In order to improve the prediction of the friction factor and provide more accurate results, we will try to find it directly from a computation of average velocity instead of the analytical approach.

5 Friction factor based on average velocity

5.1 Law-of-the-wall method

This method is based on linear and logarithmic velocity laws. The friction factor f is obtained by the average velocity (equation 2). The average velocity is obtained by integrating the linear profile until $y^+=11.5$ and the logarithmic profile for $y^+>11.5$. MATLAB provides the result directly with the "quad" function which uses recursive adaptive Simpson quadrature. Table (3) presents the results: q_1 is the result of the first integral related to the linear profile and q_2 the second one for the logarithmic velocity profile.

Table 3. Friction factor obtained by the law-of-the-wall method.

Re_τ	q_1	q_2	$q= q_1+ q_2$	u^+_{moy}	Re	$fx10^{-3}$
109	66.12	1451.9	1518.02	13.92	3036.05	10.311
150	66.12	2155	2221.12	14.80	4442.25	9.121
298	66.12	4890.4	4956.52	16.63	9913.0296	7.229
642	66.12	11882	11948.12	18.61	23896.25	5.774
2003	66.12	42978	43044.12	21.48	86088.25	4.330

Figure (6) presents the friction factor as a function of the Reynolds number obtained by the law of-the-wall method. This result is compared to DNS data and the recalibrated Dean's correlation. For $Re_\tau>395$, the results from the law-of-the-wall method are in good agreement with DNS data and therefore improve results from the former analytical methods. However for low Re, this method presents less accuracy (figure 6). This is probably due to the inaccurate prediction of the linear and logarithmic velocity profiles for low-Re (figure 5.b). For $Re_\tau=109$, the intersection of the DNS data and the log-profile seems about $y^+=20$. It is possible to obtain a more accurate velocity profile for $y^+<20$ by a method based on the momentum equation and a suitable eddy viscosity profile (Absi, 2009).

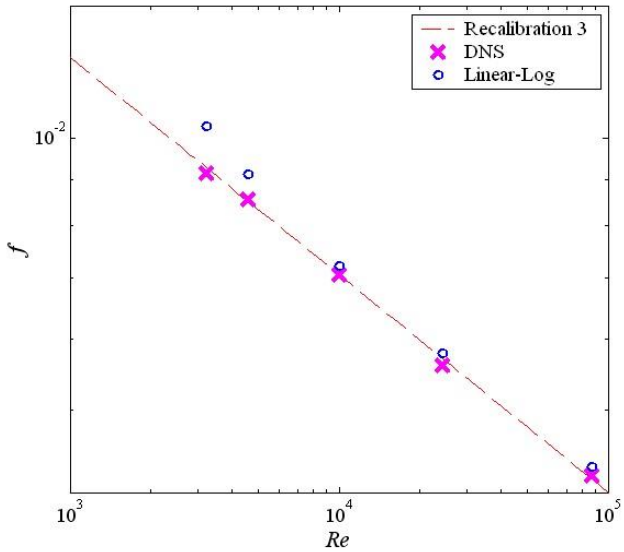

Fig. 6. Comparison of the law-of-the-wall method and DNS data.

5.2 ODE-Log method

In this method the friction factor f is obtained by the average velocity (equation 2) through two velocity profiles. The first until $y^+=20$ is obtained by a method based on the momentum equation (14) and a suitable eddy viscosity profile [3] and the second by the log-law.

$$\frac{du^+}{dy^+} = \frac{1}{1+\nu_t^+}\left(1 - \frac{y^+}{Re_\tau}\right) \tag{14}$$

In this equation, ν_t^+ represents the dimensionless eddy viscosity given by an analytical equation [5]. We can solve this equation by ODE45 function of MATLAB.
Figure (7) presents the velocity profile (red solid line) obtained by the ordinary differential equation ODE (14) for $y^+<20$ which is in very good agreement with DNS data.

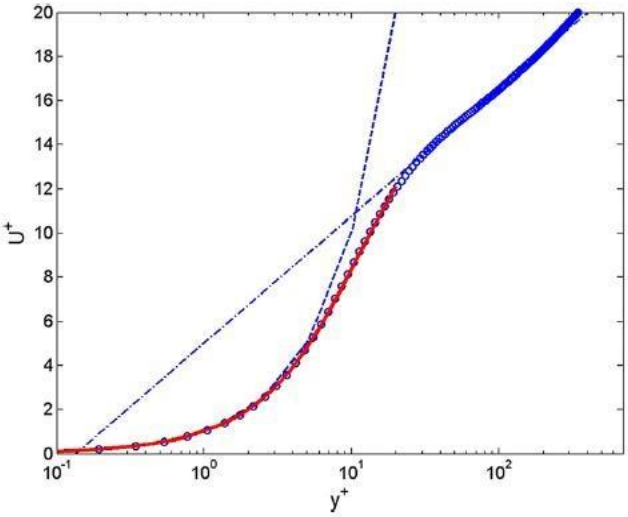

Fig. 7. Mean streamwise velocity profile $u^+ = y^+$ for $Re_\tau = 642$. for Re = 642. solid line from equation (14).

For the average velocity (equation 6), we use the trapezoidal rule for $y^+<20$ and the "quad" function for the log-law. Table (4) presents the results of *f* obtained by equation (2). Reynolds numbers are obtained by equation (3).

Table 4. Friction factor obtained by EDO-log.

Re_τ	u^+moy	Re	$f\times10^{-3}$
109	13.82	3040.80	10.468
150	14.71	4413	9.242
298	16.46	9878	7.378
642	18.58	23861.44	5.791
2003	21.51	86051.79	4.321

In order to evaluate the friction factor results obtained by the ODE-log method, we plot $f = f(Re)$ with DNS data and the results from the law-of-the-wall method (figure 8). For $Re>395$, ODE-log and law-of-the-wall (linear-log) methods provide similar results. They are in good agreement with DNS data for intermediate *Re* numbers. For low-*Re* the result from ODE-log method seems somewhat less accurate. This result is unexpected because the velocity profile obtained by the momentum equation (equation 14) is more accurate for $0>y^+>20$ and therefore the average velocity and the friction factor *f* should be improved.

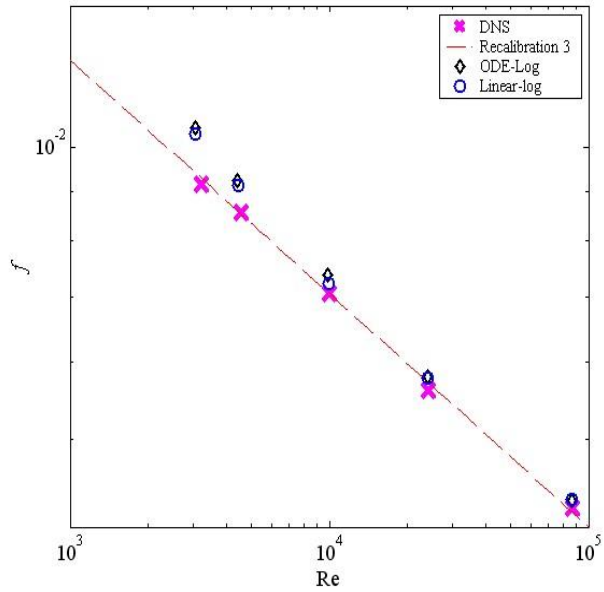

(a)

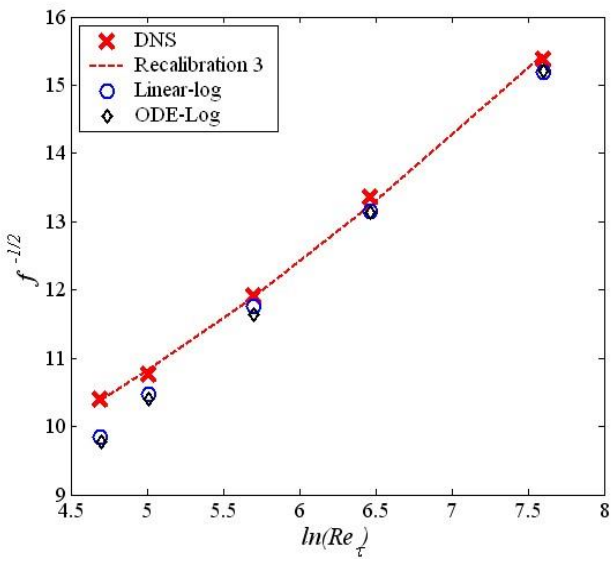

(b)

Fig. 8. Friction factor from ODE-Log and DNS data.

Figure (9) provides an explanation of this unexpected result, where for low *Re*, ODE-log method is somewhat less accurate than the law-of-the-wall method, through an analysis of the DNS data of mean velocities for $Re_\tau = 109$. Actually, both methods don't allow the balance obtained with the logarithmic friction relation (figure 5). However, the average velocity over *h* seems less accurate with the ODE-log method because it doesn't take into account the region represented by horizontal lines (figure 9).

For low-*Re*, figure (9) shows that the log-law (with κ=*0.4* and *B=5*) is unable to predict DNS data. This was also observed by Moser *et al.* for DNS where data at Re_τ=180 has almost no

log layer (Moser, Kim, & Mansour, 1999). Therefore in order to provide accurate friction factor, it is important to predict velocities accurately on the overall height *h*. Accurate velocities for $0>y^+>20$ don't allow appropriate values of *f* without a suitable velocity profile in other layers. For high *Re*, both velocities for $0>y^+>20$ and log-law are suitable. However, the velocity profile is inaccurate in the outer region for high y^+ (figures 1 and 7).

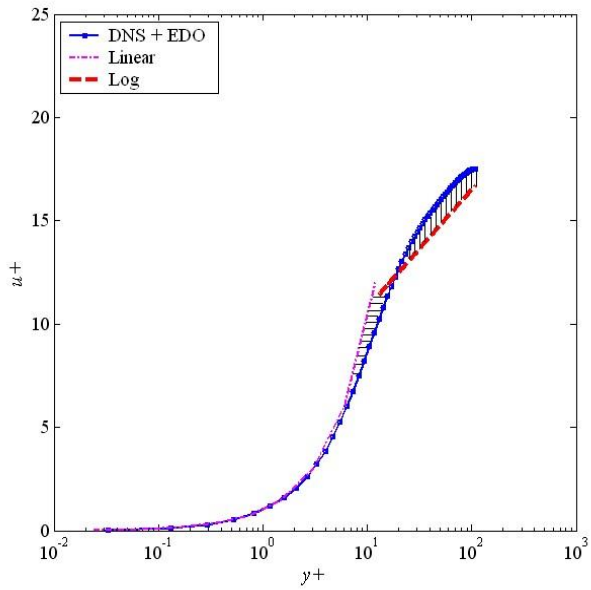

Fig. 9. Analysis of mean streamwise velocity profile for Re_τ=109

5.3 ODE-wake method

The results for f presented in the former sections show that the accuracy of velocity profile affects directly the average velocity and therefore the friction factor values. Since, experiments and DNS show that the logarithmic law is not suitable in the outer region for high y+, it is important to use a more appropriate description of velocities. Log-wake law seems more suitable, the velocity profile is given by [12-18]:

$$u^+ = \frac{1}{\kappa} ln(y^+) + B + \frac{2}{\kappa} \Pi \, sin^2\left(\frac{\pi}{2}\frac{y^+}{Re_\tau}\right) \tag{15}$$

With Π is the Coles' parameter. Figure (10) shows that adding Coles wake function to the log-law allows a better description of DNS data for high y^+. We use for the Coles' parameter a value of Π equal to 0.14 [13].

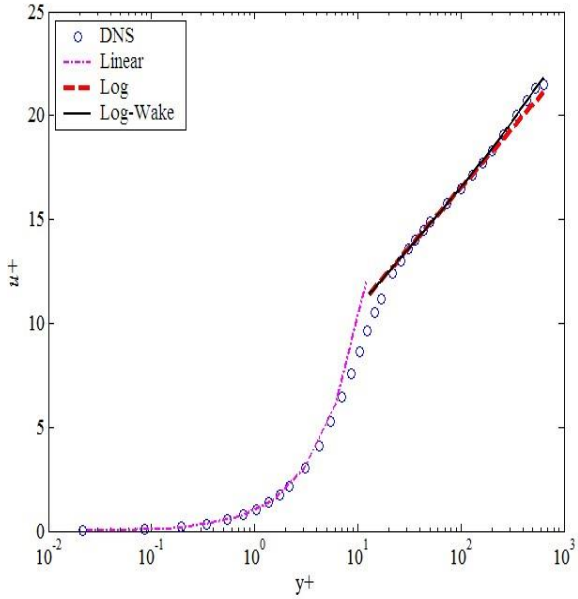

Fig. 10. Mean streamwise velocity profiles for Reτ=109; Solid line: Log-Wake Law

For the average velocity (equation 6), we use the trapezoidal rule for $y^+<20$ and the "quad" function for the log-wake law. Table (5) presents the results of *f* obtained by equation (2). Reynolds numbers are obtained by equation (3).

Table 5. Friction factor obtained by EDO-wake.

Re_τ	u^+moy	*Re*	$fx10^{-3}$
109	14.16	3088.76	9.96264
150	15.05	4517.60	8.81976
298	16.92	10086.41	6.98312
642	18.93	24309.44	5.57969
2003	21.83	87451.79	4.19676

With this correction, the friction factors obtained by both ODE (equation 14) and the log-wake law (equation 15) present the better agreement with DNS data (figures 11 and 12). Even if we improve the friction factor, inaccurate values remain at low-*Re*. This is due to the velocity profile (figure 9), where classical laws seem unable to predict DNS data. Appropriate methods to predict velocity profiles at low-*Re* numbers are therefore needed.

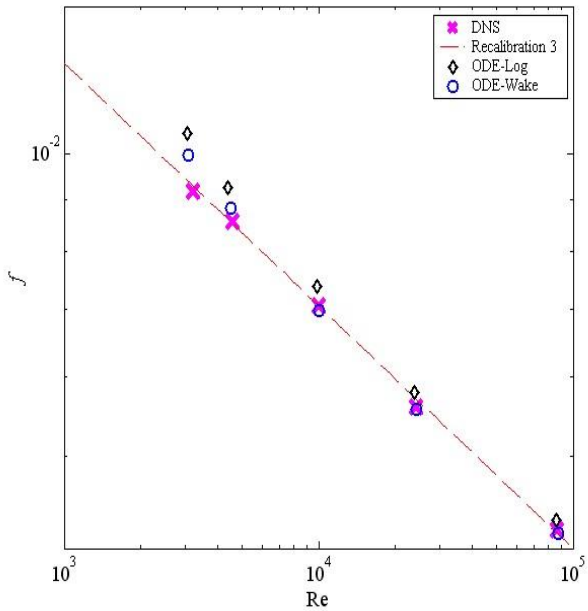

Fig. 11. Friction factors from the Log-Wake law and comparison with DNS and Law-of-the-wall method.

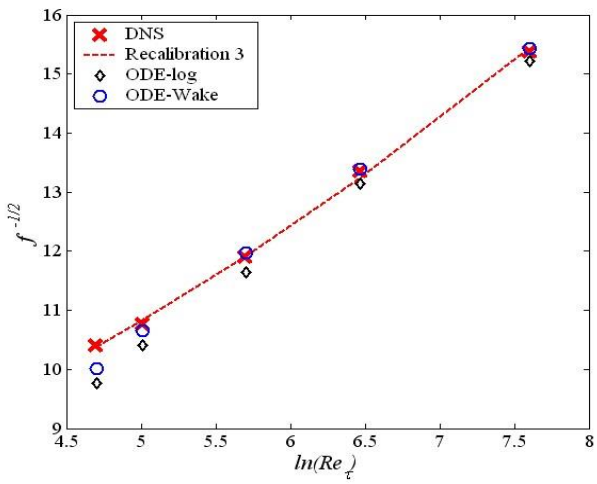

Fig. 12. Friction factors from the Log-Wake law and comparison with DNS and Logarithmic friction relation.

In order to improve inaccurate values for the friction factors at low-*Re*, we need a more appropriate description of velocities. Figure (13) shows that for $Re_\tau = 109$, ODE (equation 14) and a log-law with $\kappa = 0.4$ and a modified value of *B* equal to *6*, allows better agreement with DNS data. We obtain from these velocities a very accurate value of the friction factor (red square in figure 14).

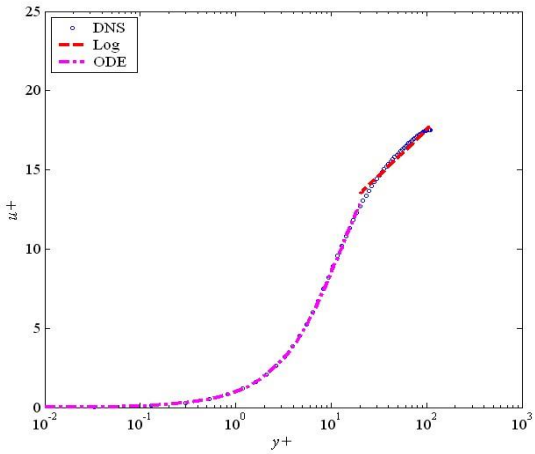

Fig. 13. Mean streamwise velocity profile for Re_τ=109, ODE and Log-law with κ=0.4 and B=6.

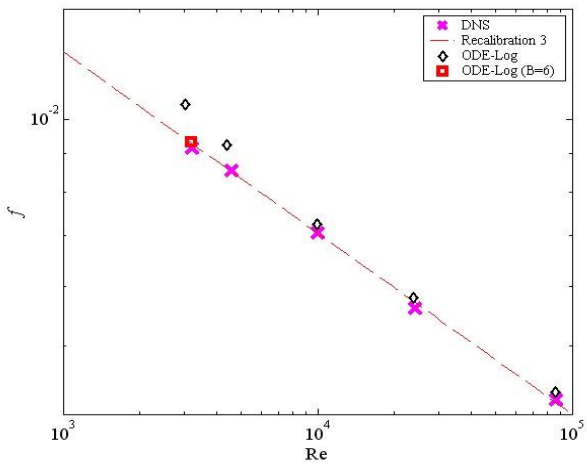

Fig. 14. Friction factor from ODE-Log with κ=0.4 and B=6 for Re_τ=109 and DNS data.

6 Conclusions

We started this study by the evaluation of Dean's correlation for the friction factor f by DNS data. We observed that it presents a gap particularly for low-Re. We proposed therefore a new calibration by DNS data. The aim of the study was to obtain more accurate wall friction factors from velocity profiles. On the one hand, we determined analytical relations for the friction factor based on velocity laws; on the other hand we obtained f from the average velocity. By assuming a logarithmic velocity profile on the overall height, we obtained a logarithmic friction relation similar to that of pipes. With this relation, f values are accurate for intermediate Re_τ, however for low and high Re_τ we observed a gap with DNS data. In order to improve this relation, we took into account the linear profile for y^+ <11.5, we obtained the linear-logarithmic friction relation. Nevertheless, for low-Re_τ, the curve is more distant from the DNS data than the logarithmic friction relation. An explanation has been proposed based on the analysis of the velocity profile. The average velocity was first

calculated from the law-of-the-wall. The results allow a good prediction of f for $Re_\tau > 395$, it improves therefore the former results from the analytical methods. However, a gap remains for low-*Re*. It can be explained by a wrong description of the velocities from the linear and logarithmic laws for low-*Re*. Since it is possible to obtain a more 10 accurate velocity profile for $y^+ < 20$ by solving the momentum equation, we used this method in 11 order to improve f. We obtained similar results than the law-of-the-wall method for $Re_\tau > 395$. However, we observed a small gap for low-*Re*. We used the analysis of velocity profile again to explain this behavior. For low-*Re*, the log-law (with $\kappa = 0.4$ and B=5) is unable to predict DNS data. Indeed, low-Reynolds number effect in channel flows has been observed previously in different experimental and computational studies. The results for f presented by these methods show that the accuracy of velocity profile affects directly the average velocity and therefore the friction factor values. In order to provide more suitable friction factor values, it is important to predict velocities accurately on the overall height h and not only for a given layer. For high-*Re*, the velocity profile is inaccurate particularly in the outer region for high y^+. We used therefore a more appropriate method which consists to use for $y^+ < 20$ the momentum equation with an eddy viscosity formulation and the log-wake law for high y^+ values. Friction factors obtained by this method allow good agreement with DNS data. For $Re_\tau = 109$, a value of $B = 6$ improves the log-law. With 29 the momentum equation for $y^+ < 20$, the friction factor allows the better description of DNS data.

References

1. R. Absi, *Time-dependent eddy viscosity models for wave boundary layers*, In: Coastal Engineering 2000, Proc. 27th International Conference on Coastal Engineering, Billy L. Edge (Ed.), ASCE Press, ISBN 0-7844-0549-2, vol. 2, pp. 1268-1281 (2001).
2. R. Absi, Analytical solutions for the modeled k-equation, Journal of Applied Mechanics, Transactions of the ASME, American Society of Mechanical Engineers, **75**(4), 044501 (2008).
3. R. Absi, A simple eddy viscosity formulation for turbulent boundary layers near smooth walls. C.R Mecanique, Elsevier, **337**, 158-165 (2009).
4. R. Absi, An ordinary differential equation for velocity distribution and dip phenomenon in open-channel flows, Journal of Hydraulic Research, IAHR, Taylor & Francis, **49**(1), 82-89 (2011).
5. R. Absi, Eddy viscosity and velocity profiles in fully-developed turbulent channel flows. Fluid Dynamics, Springer, **54**(1), 137–147 (2019).
6. R. Absi, Analytical eddy viscosity model for velocity profiles in the outer part of closed- and open-channel flows, Fluid Dynamics, **56**(4), pp. 577–586 (2021).
7. R. Absi, Reinvestigating the parabolic-shaped eddy viscosity profile for free surface flows, Hydrology, **8**(3), 126 (2021).
8. R. Absi, C. Di Nucci On the accuracy of analytical methods for turbulent flows near smooth walls, Comptes Rendus Mecanique, Académie des Sciences, Elsevier, **340**(9), 641-645 (2012).
9. G. Alfonsi and L. Primavera, The structure of turbulent boundary layers in the wall region of plane channel flow. Proc. R. Soc. A, **463**, 593-612 (2007).
10. G. Barenblatt, *Scaling* (Cambridge University Press, 2003).
11. A. Bilgil and H. Altun, Investigation of flow resistance in smooth open channels using artificial neural networks. Flow Measurement and Instrumentation, **19**, 404-408 (2008).

12. D. Coles, The law of the wake in turbulent boundary layer. J. Fluid Mech., **1**, 191-226 (1956).
13. R. Dean, Reynolds number dependence of skin friction and other bulk flow variables in two-dimensional rectangular duct flow. J. Fluids Eng., **100**, 215-223 (1978).
14. N. El Gharbi, R. Absi, A. Benzaoui, R. Bennacer, An improved near wall treatment for turbulent channel flows, International Journal of Computational Fluid Dynamics, Taylor & Francis, **25**(1), 41-46 (2011).
15. N. El Gharbi, R. Absi, A. Benzaoui, Effect of different near-wall treatments on indoor airflow simulations, Journal of Applied Fluid Mechanics, **5**(4), 63-70 (2012).
16. X. Fang, Y. Xu and Z. Zhou, New correlations of single-phase friction factor for turbulent pipe flow and evaluation of existing single-phase friction factor correlations. Nuclear Engineering and Design, **241**, 897–902 (2011).
17. J. C. Gibbings, On the measurement of skin friction from the turbulent velocity profile. Flow Meas. lnstrum., **7**(2), 99-107 (1996).
18. J. Hinze, *Turbulence* (McGraw-Hill, New York, 1975).
19. S. Hoyas and J. Jimenez, Scaling of velocity fluctuations in turbulent channels up to Reτ=2003. Phys. of Fluids, **18**, 011702 (2006).
20. K. Iwamoto, Database of fully developed channel flow,. THTLAB Internal Report No. ILR0201, Dept. Mech. Eng., Univ. Tokyo. Tokyo (2002).
21. D. D. Joseph and B. H. Yanga, Friction factor correlations for laminar, transition and turbulent flow in smooth pipes. Physica D, **239**, 1318-1328 (2010).
22. F. Laadhari, On the evolution of maximum turbulent kinetic energy production in a channel flow. Physics of Fluids, **14**(10), L65-L68 (2002).
23. P. Li, J. E. Seem and Y. Li, A new explicit equation for accurate friction factor calculation of smooth pipes. International Journal of Refrigeration, **34**, 1535-1541 (2011).
24. B. McKeon, C. Swanson, M. Zagarola, R. Donnelly and A. Smits, Friction factors for smooth pipe flow. J. Fluid Mech., **511**, 41-44 (2004).
25. B. McKeon, M. Zagarola and A. Smits, A new friction factor relationship for fully developed pipe flow. J. Fluid Mech., **538**, 429-443 (2005).
26. R. Moser, J. Kim and N. Mansour, Direct numerical simulation of turbulent channel flow up to Ret5590. Physics of Fluids, **11**(4), 943-945 (1999).
27. M. M. Rahman and T. Siikonen, An eddy viscosity model with near-wall modifications, Int. J. Numer. Meth. Fluids, **49**, 975–997 (2005).
28. T. Wei and W. Willmarth, Reynolds-number effects on the structure of a turbulent channel flow. J. Fluid Mech., **204**, 57-95 (1989).
29. M. Welderufael, R. Absi, Y. Mélinge, Assessment of velocity profile models for turbulent smooth wall open channel flows, ISH Journal of Hydraulic Engineering, Taylor & Francis. **28**(sup1), 69-79 (2022).
30. E.-S. Zanoun, F. Durst and H. Nagib, Evaluating the law of the wall in two-dimensional fully developed turbulent channel flows. Physics of fluids, **15**(10), 3079-3089 (2003).